Scientific Research Publishing

Open Journal of Geology, 2026, 16(1), 52-72
https://www.scirp.org/journal/ojg
ISSN Online: 2161-7589
ISSN Print: 2161-7570

Mechanical Response Analysis of the Pile Foundation of the Shield Undercutting Replacement Bridge

Haijun Zhou[1], Hui Lu[2*], Fengjiang Luo[3]

[1]China Jiangsu Sci-Tech Innovation Industry Development Co., LTD, Nanjing, China
[2]Research Center of Urban Underground Space, Nanjing Tech University, Nanjing, China
[3]China Railway 24th Bureau Group Co., LTD, Shanghai, China
Email: *3110375587@qq.com

How to cite this paper: Zhou, H.J., Lu, H. and Luo, F.J. (2026) Mechanical Response Analysis of the Pile Foundation of the Shield Undercutting Replacement Bridge. *Open Journal of Geology*, **16**, 52-72.
https://doi.org/10.4236/ojg.2026.161004

Received: December 30, 2025
Accepted: January 27, 2026
Published: January 30, 2026

Abstract

As a typical representative of the application of urban underground space, subway lines inevitably conflict with the foundations of existing buildings (structures). In this paper, in order to solve the problem of cross conflict between the shield tunnel and the pile foundation of existing bridges, with the background of an actual buttressing project, the finite element method was used to establish a model of the buttressing pile foundation of a bridge under a shield tunnel. Then, numerical simulation analysis was carried out on the basis of the model of the buttressing pile foundation of existing bridges under the shield tunnel, which includes surface settlement, vertical displacement of the bridge surface, displacement of the original pile and static pile caused by shield tunnel construction of the right line of the tunnel. The changes of pile axial force and the stress response of the buttress beam are analyzed and discussed, and the following conclusions are obtained: Firstly, the peripile frictional resistance of the pile foundation has a certain inhibiting effect on the reduction of soil settlement due to the influence of tunnel construction. Secondly, the beams and cover beams can play a certain role in the deformation coordination during the construction process. Again, in the process of shield tunneling, under the influence of tunneling pressure and grouting pressure, the original piles and hydrostatic piles will produce certain bending deformation in space. Finally, in the process of shield driving, the soil above the tunnel will settle downward, which will lead to the generation of negative frictional resistance under the influence of the coordinated deformation of the bearing platform and the remaining pile.

Keywords

Pile Buttressing Technique, Shield Tunnel Construction, Numerical

Simulation, Bridge Pile Foundation, Underpassing

1. Introduction

With the development of urban subway systems, tunneling through existing buildings has become an unavoidable engineering problem [1]. The pile foundation replacement technology was first used in the construction of the New York subway [2]. It can effectively solve the problem of shield tunnels passing under existing buildings and structures. Furthermore, with the development of computer technology, numerical simulation is widely used to solve shield tunneling problems [3] [4].

Makarchian *et al.* [5] proposed a simple method for designing support piles by utilizing the interaction between piles and rafts. They optimized the pile foundation underpinning design scheme through finite element numerical analysis and compared the simplified analysis results with the corresponding actual engineering monitoring data to verify its reliability. Jin Fangfang *et al.* [6] used the pile foundation replacement project of a section of Shanghai Metro Line 10 to point out the reasonable excavation exposure length in the pile foundation replacement process by combining theoretical calculation and numerical simulation. Vynnykov *et al.* [7] proposed a reinforcement scheme that integrates existing pile foundations into reinforcement measures to address the problem of excessive foundation deformation and the inability of pile ends to reach the design depth. They also estimated the safety of this new system using the finite element method. Zhao *et al.* [8] relied on the pile foundation conflict replacement project of Shenzhen Metro Line 12, adopted the active replacement technology of irregular pile cap for replacement, and analyzed the safety of irregular pile cap replacement through numerical simulation. Ma *et al.* [9] introduced the key issues of pile foundation replacement based on a subway tunnel project, and calculated the bearing capacity of a single pile and the deformation of the replacement beam. The bearing capacity of a single pile was calculated by numerical simulation to verify the feasibility of the pile foundation reinforcement scheme. Xu *et al.* [10] proposed a construction scheme for the underpinning of enlarged slab foundation and shield pile cutting based on the engineering case of shield tunnel crossing pile foundation of Shanghai Metro Line 10. They also adopted a combination of theoretical analysis and numerical simulation to study the transformation law of structural stress during the underpinning process. Li *et al.* [11] used numerical simulation to study the stress effect of foundation pit excavation on the underpinning piles in the area, based on the Zhengzhou 107 Auxiliary Road Rapid Transit Project. Deng *et al.* [12] relied on the active replacement of the pile foundation of the shield tunnel under Xima Bridge of Fuzhou Metro Line 1, and used the method of combining numerical simulation and field measurement data to analyze the internal force and displacement response of the bridge structure under different loads for the

complex statically indeterminate structure composed of the bridge superstructure, pile body, and soil. The results were consistent with the measured data. Zhang *et al.* [13] relied on a subway shield tunnel crossing an urban overpass pile foundation replacement project and adopted a combination of numerical simulation and on-site monitoring to obtain a suitable pile foundation replacement construction scheme. Cheng *et al.* [14] conducted numerical simulations of the entire pile foundation underpinning project and explored the load transfer mechanism of the bridge system. Richard P. Stulgis [15] used the pile foundation load test method in the St. Joseph's Charitable Hospital project to explore the settlement problem of the building during the underpinning process of small pile foundations and monitored the settlement of the building after the underpinning construction. Horpibulsuk *et al.* [16] took the replacement project of the student dormitory at Suranare University of Technology in Thailand as a case study. Based on the test results of the foundation soil, they gave the replacement design and its construction process, and verified the rationality of the design scheme through subsequent monitoring. Ishimura *et al.* [17] developed a new method for demolishing pile foundations of existing structures by using a wire saw system to horizontally cut the piles below the existing structure. This method is safer and less costly than traditional methods because it does not require underground work or ground modification. Van Hasselt D *et al.* [18] described the defining features of the Amsterdam Metro, such as the presence of pile foundations, tunneling technology, and deep underground stations. Iwasaki Y *et al.* [19] introduced the Nagoya subway project in Japan, which uses cast-in-place concrete pile support for a large underground structure. Due to the geological and construction conditions at the project site, the piles had to be designed as friction piles. Yamaguchi I *et al.* [20] studied four closely connected subway tunnels built in Yokoto, Japan. During the planning and design phase before construction, the problems associated with closely connected tunnels were studied. Various monitoring during the construction phase resulted in the collection of a large amount of data, including load transfer between the tunnels and ground characteristic behavior during the construction of the four tunnels. In order to improve the evaluation method of close-proximity tunnel interaction, it is attempted to analyze and evaluate the behavior of tunnels and surrounding ground using the data obtained from the above projects.

However, research on pile foundation replacement needs further development, especially regarding the mechanical response of bridge pile foundations after shield tunneling under the replacement system. Therefore, this paper takes the pile foundation treatment project of the Nanjing Metro Line 3 Phase III, between Mozhou East Road Station and Moling Street Station, under the Dongwang Bridge as an example. Using the finite element method, it analyzes the mechanical response characteristics and differences between the original bridge structure and the replacement system during the shield tunneling process. Furthermore, it analyzes and discusses the surface settlement, vertical displacement of the bridge

deck, displacement of the original piles and static pressure piles, changes in pile axial force, and stress response of the replacement beam caused by the right-line shield tunneling.

2. Shield Tunneling under Bridge Pile Foundation Replacement Scheme

2.1. Engineering Background

After departing from the shield tunnel shaft, the tunnel proceeds south along Shuanglong Avenue, passing under Dongwang Bridge. Dongwang Bridge is located between Mozhou East Road Station and Moling Street Station on Nanjing Metro Line 3 Phase III, and is part of Shuanglong Avenue. The Nanjing Metro Line 3 route design shows that four bridge abutment piles from Dongwang Bridge intrude into the tunnel, two on each of the left and right lines. The positional relationship between the shield tunnel and the intruding bridge abutment piles is shown in Figure 1 and Figure 2.

The Dongwang Bridge has a clearance of only 2.2 meters between its base and the riverbed, limiting construction space and preventing large machinery from accessing the site. Furthermore, a still river flows beneath the bridge, necessitating the construction of a cofferdam to prevent leakage and ensure progress. Construction involves excavation of the bridge piers, requiring strict adherence to river water quality standards and prohibiting pollution. Due to the limited space beneath the bridge, large steel pipe piles cannot be transported; instead, they must be welded and spliced in smaller sections to reach the designed pile length. Throughout the construction process, every step must ensure that the bridge structure, road surface settlement, and surrounding pipelines meet design requirements, making the construction process complex and challenging.

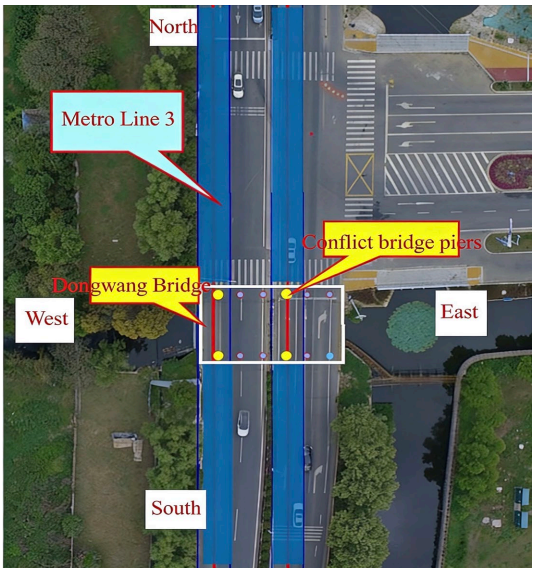

Figure 1. Planar location map of the shield line and the conflicting bridge pile.

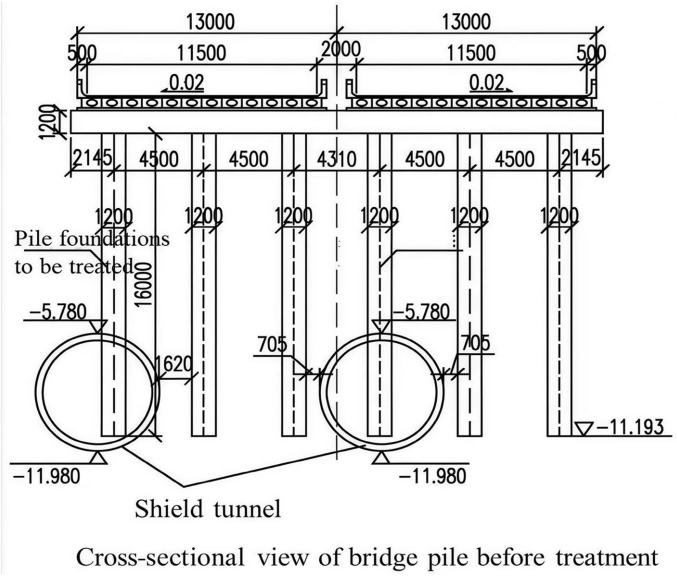

Figure 2. Profile of the shield tunnel relative to Dongwang Bridge.

2.2. Bridge Pile Foundation Replacement Scheme

The pile foundations of Dongwang Bridge that conflicted with the shield tunnel were replaced. Excavation was carried out to the design elevation, and two L-shaped replacement beams were constructed under the bridge cap beams on both sides. Static pressure piles were then constructed on the replacement beams to complete the bridge replacement and achieve load transfer. Figure 3 shows the cross-sectional view of Dongwang Bridge after the treatment. To ensure construction safety, grouting reinforcement was carried out behind the abutments before constructing new support beams and replacement pile foundations. The load borne by the pile foundations that needed to be removed due to the shield tunneling was ultimately transferred to the newly constructed replacement pile foundations through the new support beams. The overall construction process of Dongwang Bridge is shown in Figure 4.

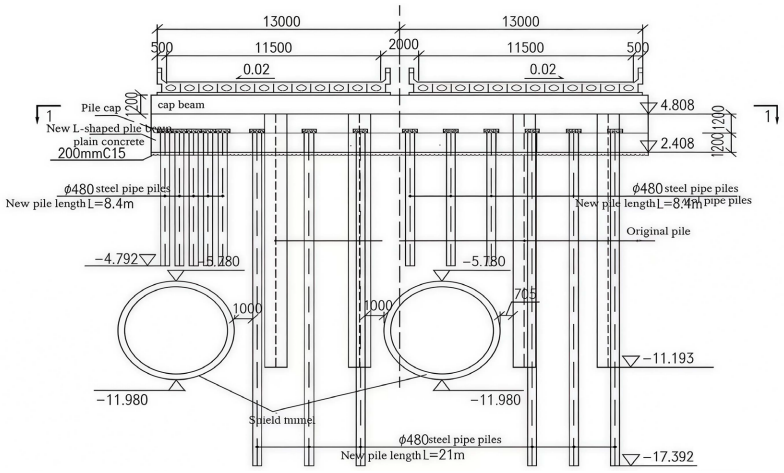

Figure 3. Cross-section of Dongwang Bridge after treatment.

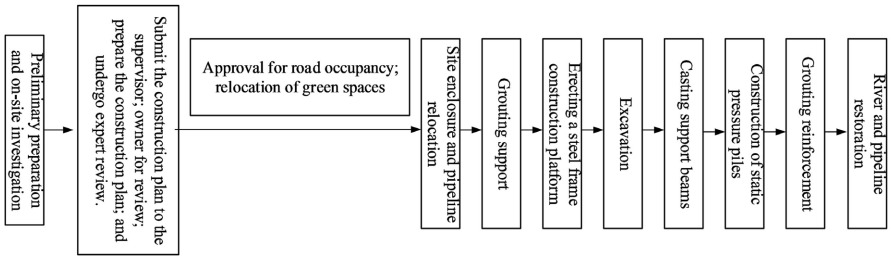

Figure 4. Overall construction flow chart of Dongwang Bridge.

2.3. Numerical Simulation of Pile Foundation Underpinning

This paper uses the finite element method and selects the modified Mohr-Coulomb constitutive model for three-dimensional numerical simulation analysis.

1) Simplified calculation of the model

Both shield tunneling and pile foundation replacement are complex dynamic construction processes. In the simulated construction process, some assumptions were first made, the main contents of which are as follows:

a) The main consideration for this project is the impact of the underpinning construction on the original bridge-pile system. Since there are no complex buildings in the surrounding area, the model size is 90 m*110 m*70 m to simulate the impact of the construction on the surrounding environment.

b) Before the pile foundation replacement construction, the surrounding river was cut off. The numerical model does not consider the influence of surface water; instead, an equivalent water load is added to the model as a substitute.

c) There is a slope of about 1 m on the side of the bridge. When considering the terrain, the soil is approximated as a regular rectangular block.

d) The bridge deck, cap beams, newly built abutments, original bored piles, and newly built steel pipe piles are all treated as ideal linear elastic materials, and the soil is evenly distributed in layers.

2) Model dimensions and related parameters

A three-dimensional model was established based on the actual site environment. To fully consider the impact of pile foundation replacement construction and subsequent shield tunneling on the surrounding environment, the overall model size was taken as four times the pile length, with slight increases and decreases in different directions. The model dimensions were 110 m in the shield tunneling direction (Y direction), 90 m on both sides of the model boundary (X direction), and 70 m in the model depth (Z direction). Taking into account the location relationships on site, the established three-dimensional model was 90 m*110 m*70 m, as shown in Figure 5 below.

Based on the geological survey report and experimental data of the subway and Fenglu Station, the soil layers in the model are divided into 7 categories. The soil layer types and their physical and mechanical parameters are shown in Table 1.

The modified Mohr-Coulomb constitutive model also contains three important nonlinear stiffness parameters: tangent stiffness from the principal compaction loading test E_{oed}^{ref} secant stiffness from the triaxial test E_{50}^{ref} (secant stiffness

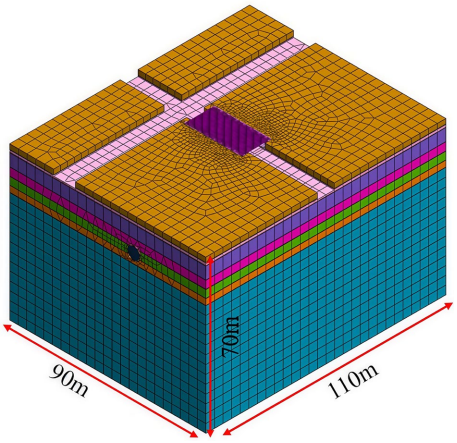

Figure 5. Schematic of the overall dimensions of the model.

Table 1. Soil parameters of the constitutive model.

Site soil layers	μ	φ/°	c/kPa	γ/kN·m^3	E_s/MPa	E_{oed}^{ref} /MPa	E_{50}^{ref} /MPa	E_{ur}^{ref} /MPa	Layer thickness/m
Miscellaneous fill	0.30	25	5	22	4.5	4.5	4.5	13.5	2.3
Silty clay 1	0.30	15.8	32.7	19	6.3	6.3	6.3	18.9	1.2
silty clay	0.38	17.5	14.6	18	5.8	5.8	5.8	17.4	5.7
Silty clay 2	0.30	17.4	48.8	20	9.1	9.1	9.1	27.3	3.7
Silty clay 3	0.32	16.9	36.5	20.1	9.3	9.3	9.3	27.9	3.6
Silty clay 4	0.30	17.0	45.6	20	13.4	13.4	13.4	40.2	2.8
medium and fine sand	0.30	34.1	4.5	20.2	12.9	12.9	12.9	38.7	4.7

from the standard drained triaxial test) and unloading elastic modulus E_{ur}^{ref} (elastic modulus under elastic unloading/reloading). Based on engineering experience, these can generally be taken as $E_{oed}^{ref} = E_{50}^{ref} = nE_s = E_{ur}^{ref}/3$, n is taken as 0.9 - 1 based on experience. The tunnel structure, the original bridge pile system, and the newly constructed pile foundation system all adopt elastic constitutive models, and the structural parameters are listed in Table 2.

Table 2. Parameters of the elastic constitutive model for structures.

Structure name	E/GPa	μ	γ/kN·m^3	Unit type
steel pipe piles	208	0.28	78.5	1D beam element
New pile caps and girders	30	0.2	26	3D entity
Bridge deck	30	0.2	26	2D board unit
Original pile	30	0.2	26	1D beam element
Shield	250	0.25	78	2D board unit
Shield tunnel segments	38	0.28	25	2D board unit
Grouting layer	13	0.25	20	3D entity

3) Boundary conditions and load settings

MIDAS GTS can establish boundary conditions for the model using its automatic constraint function. This function can set horizontal displacement constraints around the model (X and Y directions), set vertical displacement constraints at the bottom of the model (Z direction), and leave the top of the model unconstrained (a free surface). The model contains two rivers that run through it. To prevent excessive deformation and displacement in the river areas, normal displacement constraints were added to the soil perpendicular to the riverbanks, corresponding to the concrete slope protection of the rivers, thus better reflecting the actual situation.

After setting the model boundaries, loads need to be applied to the model. During construction, the bridge deck will be open to traffic, and bridge deck loads must be set. In the original bridge design, the road grade is Highway Class I, the load level is vehicle load −20 kN/m^2, trailer load −100 kN/m^2, and pedestrian load is 3.5 kN/m^2; the bridge pile foundation reinforcement design standard is to maintain the original load level. The standard value of the Highway Class I lane load (uniformly distributed load) is 10.5 kN/m^2. The thickness of the bridge deck fill material of Dongwang Bridge is 0.7 m (including the pavement thickness), which is greater than or equal to 0.5 m, so impact force is not considered.

In summary, the design load on the bridge deck surface is as follows:

$$q = 10.5 + 3.5 = 14 \ \text{kN/m}^2 \tag{1}$$

The tunnel boring machine (TBM) advances one ring to a depth of 1.2 m each time. To simplify calculations, the tunnel is advanced two rings at a time. The formula for calculating the jacking force at the tunnel face is:

$$F_w = k_0 \gamma h \tag{2}$$

where coefficient of earth pressure at rest $k_0 = 1 - sin\varphi$. The use of the at-rest earth pressure coefficient is primarily based on the mechanical characteristics of the soil in front of the tunnel face during the shield tunneling stage, where lateral deformation is restricted. Under the constraint of the shield shell, the soil has not yet undergone significant unloading or plastic failure; its stress state is closer to in-situ stress conditions than to active or passive earth pressure states. When the lateral strain of the soil is approximately zero, its horizontal stress can be characterized by at-rest earth pressure. Therefore, calculating the equivalent lateral pressure at the tunnel face can reasonably reflect the average constraint effect of the soil on the shield shell and excavation face during shield tunneling. The highest elevation of the shield's top plate −11.8 m, and the lowest elevation of the bottom plate is −18.0 m. Based on the soil layer information in the table above, the shield face thrust is calculated. The highest point of the shield is located in the ③-2b2-3 silty clay layer, coefficient of earth pressure at rest 0.710, resulting in earth pressure at rest $\sigma_{0\text{顶}} = k_{0\text{顶}} \sum \gamma h$ = 0.71 × 176 = 123.4 kN/m^2; The lowest point of the shield is located in the ③-3b1-2 silty clay layer, coefficient of earth pressure at rest 0.708, earth pressure at rest $\sigma_{0\text{底}} = k_{0\text{底}} \sum \gamma h$ = 0.701 × 352 = 249.22 kN/m^2.

Therefore, the shield face thrust is set as the average pressure of the surface load, which is σ = 186.3 kN/m^2.

The river load is calculated based on the water depth: 2.0 m on the east side and 1.5 m on the west side. The calculated river load on the east side is σ = 20 kN/m^2, river load on the west side σ = 15 kN/m^2. During tunnel boring, the completed tunnel segments are subjected to grouting pressure, set as load on pipe wall σ = 100 kN/m^2. Furthermore, the reaction force from the jacks applied to the segments during segment splicing is set as a uniformly distributed surface load at the segment cross-section of σ = 100 kN/m^2.

In addition, the model as a whole should be subjected to a self-weight load. Before construction, the ground stress should be balanced, and then a displacement zeroing construction step should be applied to eliminate the displacement effect caused by the initial stress balance.

3. Mechanical Response of Bridge Pile Foundation after Shield Tunneling and Underpinning

3.1. Numerical Model Establishment

The tunnel centerline is buried 14.9 m below the road surface. The shield tunnel has an outer diameter of 6.2 m and an inner diameter of 5.5 m. The tunnel structure adopts a circular double-line, double-tunnel configuration. In the actual project, the right tunnel was constructed first, and the left tunnel was constructed after the right tunnel was completed. The analysis model is the same as in Chapter 2. The geological model dimensions are 90 m*110 m*70 m (in the X, Y, and Z directions, respectively). The soil constitutive model, soil layer parameters, structural parameters, and applied loads are based on the pile foundation underpinning scheme. The positional relationship between the shield tunnel and the newly constructed pile foundation system is shown in Figure 6.

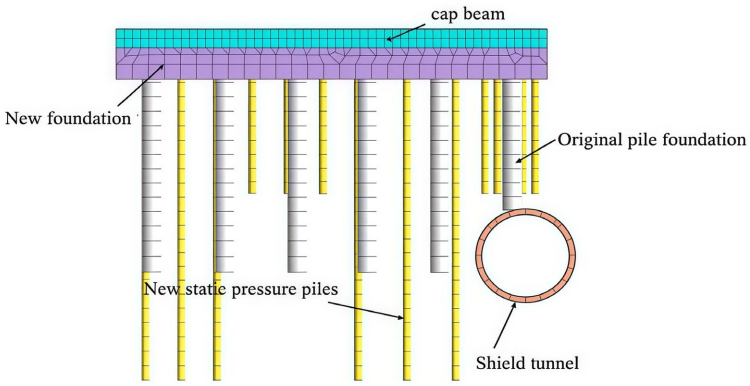

Figure 6. Spatial location map of the new supporting structure and tunnel.

This modeling was conducted after the completion of pile foundation replacement construction, followed by shield tunneling for bridge pile foundation construction. The displacement effects of pile foundation replacement were not con-

sidered, assuming the bridge structure was stable before shield tunneling. Therefore, a displacement-zeroing construction phase group was set up before shield tunneling, with the following steps:

A three-dimensional mesh element is established according to the design scheme, and the mesh soil layer parameters are assigned. Appropriate displacement boundary conditions are applied to balance the ground stresses.

a) A three-dimensional mesh element is established, soil layer parameters are assigned, and displacement boundary conditions are applied to balance the ground stress. The original bridge structure is applied, pile foundation rotation constraints are activated, bridge deck loads are applied, and a displacement zeroing step is added to eliminate the influence of soil stress balance and displacement from the original bridge construction.

b) The bridge pile foundation replacement construction was carried out, simulating the actual steps: after passivating the soil of the newly built pile cap, it was activated and its properties were changed to simulate the completion of the construction of the new pile cap; the steel pipe pile unit and the rotational constraint of the pile were activated.

c) The pile cutting simulation was used to passivate the simulated truncation of the pile foundation unit under the newly built pile cap, and then the displacement zeroing stage was established to isolate the cross-influence of the displacement of the shield tunnel and the pile foundation underpinning stage.

d) The right-line tunnel of the shield tunnel was excavated to the breakthrough-specific boundary condition in the modeling sequence. Shield segments and grouting layers were pre-set. The segments, 0.35 m thick, were 2D plate units, spliced by activation and passivation. The grouting layer was constructed by changing the unit properties. The shield machine was 7.2 m long, with a depth of 1.2 m per ring. The excavation steps were as follows: applying face excavation pressure and shield machine shell, passivating the tunnel soil and grouting layer units; after excavating 7.2 m, activating the segments and grouting layer units and changing their properties, activating the grouting pressure and jack pressure, and passivating the shield machine shell units and the pressure from the previous step; repeating this process until the tunnel was completed.

In the MIDAS GTS NX finite element software, pile cutting is typically achieved through element deactivation. During a specified construction phase, the corresponding solid or beam elements are removed from the global stiffness matrix, preventing them from participating in subsequent calculations. Passivation is usually achieved by significantly reducing the stiffness parameters of the pile foundation material or simultaneously weakening the strength parameters of the pile-soil interface elements. Regardless of whether element deactivation or a sudden stiffness drop is used, load transfer numerically appears instantaneous.

3.2. Numerical Model Establishment

3.2.1. Surface Subsidence

The simulation involved a right-line tunnel boring machine (TBM) passing under

a bridge and replacing its pile foundations until complete tunneling. The soil above the TBM experienced stress release and vertical deformation. Displacement cloud maps at different stages of the TBM's passage through the bridge show that the TBM's excavation disrupted the soil stress balance. After complete tunneling, the maximum settlement of the soil directly above the tunnel was 8.7 mm, while the maximum rebound directly below was 11.7 mm. Numerous monitoring and numerical studies of shield tunneling construction in urban subways have shown that, under similar geological conditions and burial depths, the surface settlement or rebound caused by shield tunneling is quite close to the simulation results, with errors within acceptable limits. Numerical simulation results show that the maximum surface rebound after shield tunneling is 11.7 mm, slightly larger than the maximum settlement of 8.7 mm. This phenomenon is mainly related to the unloading-reloading stiffness parameter in the constitutive model used. The unloading modulus is usually significantly larger than the secant modulus during the loading stage, reflecting the strong elastic recovery ability of the soil during stress unloading. Therefore, when shield tunneling causes stress release in the strata, the soil may exhibit significant rebound deformation, the amplitude of which can be greater than the settlement formed during the loading stage under certain conditions. Furthermore, Nanjing Metro Line 3 is mainly composed of cohesive soil, which typically exhibits significant elastic rebound characteristics under unloading conditions. The shift in stress path from loading to unloading during shield tunneling, combined with the higher unloading stiffness parameter, leads to a relatively large surface rebound amplitude. To investigate the surface settlement pattern, three sections were taken: the edge of the bridge deck, 12 m from the bridge deck, and 40 m from the bridge deck. Plots were created with the right endpoint of the model as the origin and the horizontal direction as the X-axis. The results are shown in Figure 7.

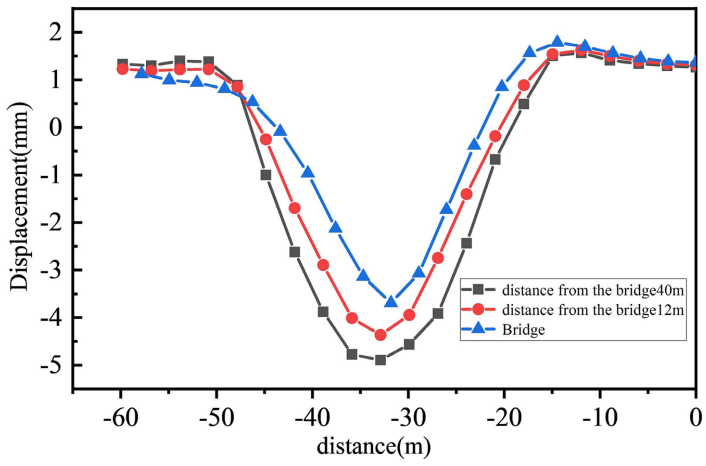

Figure 7. Vertical displacement map of the surface in different sections.

3.2.2. Vertical Displacement of the Bridge Deck

Using the bridge deck displacement cloud map, three positions were selected on

the right side of the bridge deck along the shield tunneling direction: the lower right end point, the center line, and the upper right end point, designated as D1, D2, and D3 respectively (as shown by the red dots in Figure 8). The vertical displacement curves were plotted for the three stages from the first pile grinding (21 rings) to the second pile grinding (26 rings), and finally to the complete penetration of the model by the right line (48 rings), showing the variation in vertical displacement with the number of shield rings.

As shown in Figure 8, after the shield tunneling cuts the piles, the bridge deck continues to settle, and the soil enters a long consolidation and settlement process until a new equilibrium is reached. The shield tunneling construction disrupts the original soil stress field, and the new bridge-pile system and the surrounding soil need a certain amount of time to re-equilibrate and form a new stress equilibrium field, eventually reaching a new stable state.

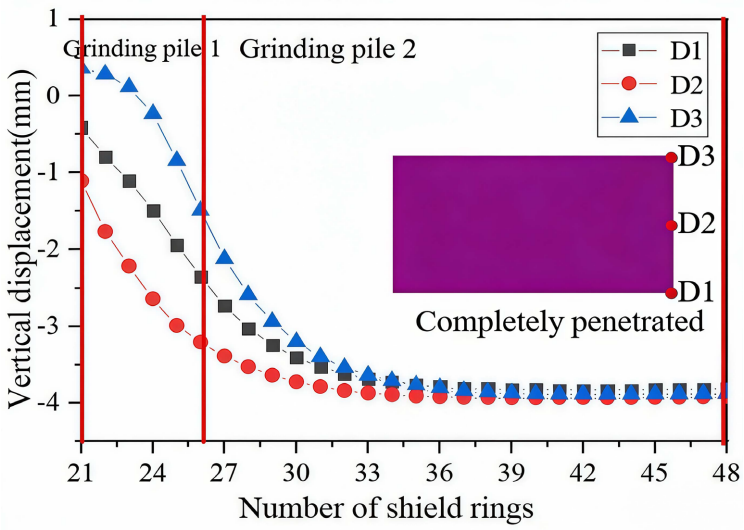

Figure 8. Vertical displacement diagram of different point positions of the bridge deck as they change with the number of shield driving rings.

3.2.3. Horizontal Displacement of the Original Pile

Figure 9 shows the horizontal displacement of the original piles in three stages: before the shield tunnel passes through the bridge, after it passes through the bridge, and after the model is fully penetrated. Comparing Figure 9(a) and Figure 9(b), the lateral deformation of piles P1-P6 increases during the second pile grinding, indicating that the second pile grinding has a cumulative effect on bridge deformation. As the original piles P1-P6 move further away from the shield tunnel, the lateral displacement of P2-P6 decreases, with piles closer to the tunnel being more affected. Due to the diffusion and transmission of shield tunneling pressure and the additional force from the cutterhead, the deformation of the original piles is caused by the pressure diffusion of the shield tunneling and the additional force from the cutterhead. P1 on the right side is directly above the tunnel and intrudes into it, so it shifts to the left and deflects under stress.

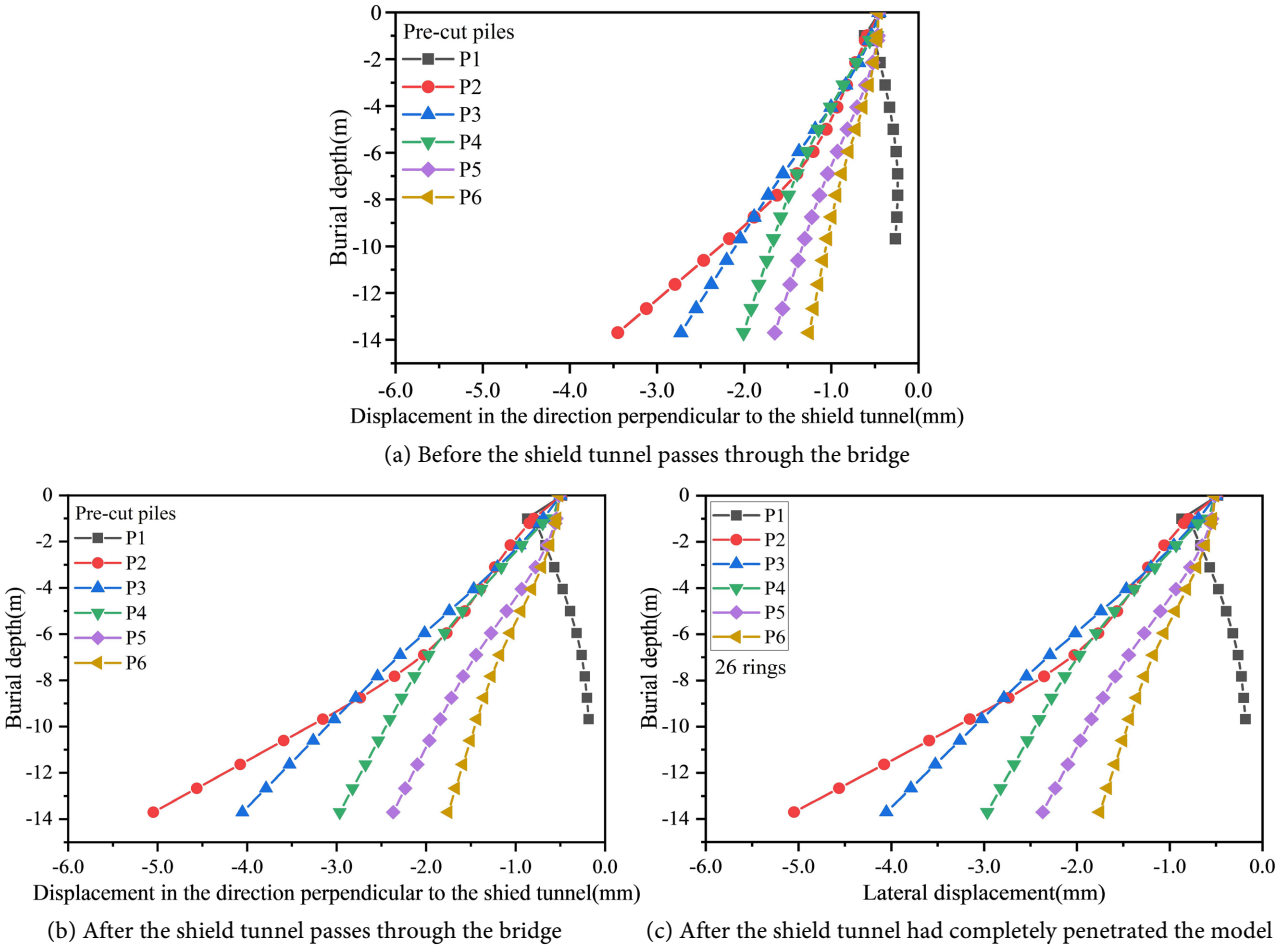

(a) Before the shield tunnel passes through the bridge

(b) After the shield tunnel passes through the bridge

(c) After the shield tunnel had completely penetrated the model

Figure 9. Lateral displacement map of the original pile at different shield stages.

As shown in Figure 9(c), after the shield tunnel passes through the pile foundation, the pile foundation still exhibits a very small degree of lateral deformation increment, with a maximum deformation increment of 0.3 mm. The main reason for this is that after the shield tunnel passes through the bridge, the soil stress is released, the overburden soil above the tunnel settles downward, and the pile cap undergoes a certain degree of deflection. Under the joint coordination of the cap beam and the pile cap, the original pile foundation will undergo a certain degree of coordinated deformation, resulting in a small lateral deformation.

3.2.4. Deformation of Newly Constructed Steel Pipe Piles

Figure 10 shows the lateral displacement (perpendicular to the tunneling direction) of the long static pressure piles at three stages of shield tunneling: ring 21, ring 26, and ring 48 (the first pile grinding stage, the second pile grinding stage, and the tunnel penetration stage). Comparative analysis shows that the second pile grinding stage has the greatest impact on the static pressure piles, with a maximum lateral displacement of approximately 4.6 mm. As the shield moves away from the supporting pile foundation, the static pressure piles undergo slight deformation due to grouting pressure, with a maximum additional increase of ap-

proximately 0.3 mm, which has little impact on the overall spatial position of the piles. Furthermore, it can be observed that the long static pressure piles experience significant flexural deformation due to the tunneling pressure and the compression of the surrounding soil during shield construction. The impact of shield tunneling on the static pressure piles decreases with increasing distance, with the affected area being approximately 0.7 times the tunnel depth.

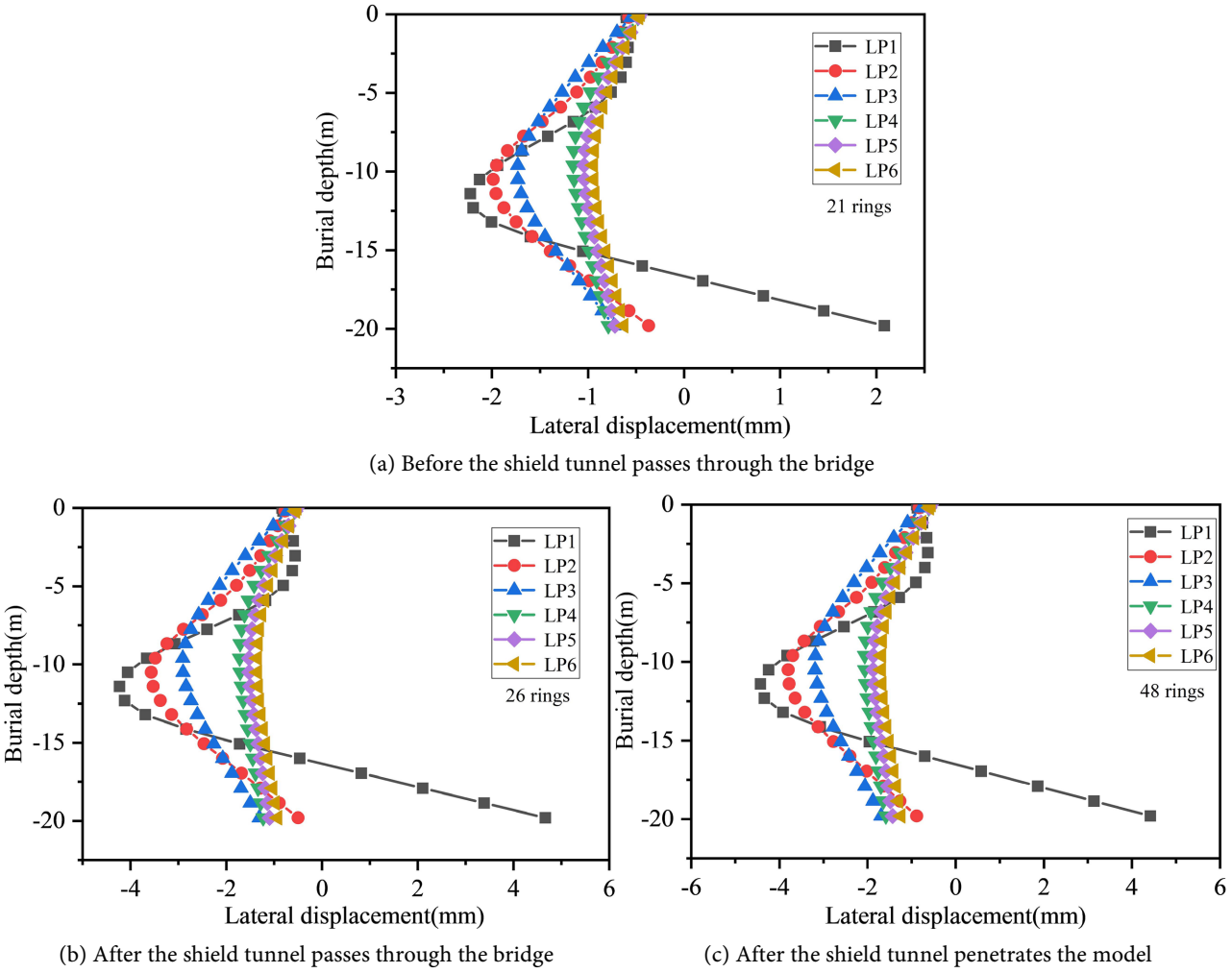

(a) Before the shield tunnel passes through the bridge

(b) After the shield tunnel passes through the bridge

(c) After the shield tunnel penetrates the model

Figure 10. Lateral displacement diagram of a long static pile at different stages of shield.

Figure 11 shows the displacement of the static pressure piles at different stages in the tunneling direction. Influenced by the tunnel boring machine's pressure, the displacement in this direction is consistent with the lateral displacement, with significant flexural deformation near the tunnel. Comparing the three stages, the displacement changes of static pressure pile LP1 differ. Before tunneling, the middle of the pile bulges due to the pressure of the jacking soil; during tunneling, the tunnel face moves away from the pile position, and the pile bottom experiences large displacement due to unloading during excavation; when the pile passes through completely, the pile bottom displacement decreases, and the flexural de-

formation slightly recovers. Other replacement piles show similar displacements, varying depending on their distance from the tunnel boring machine.

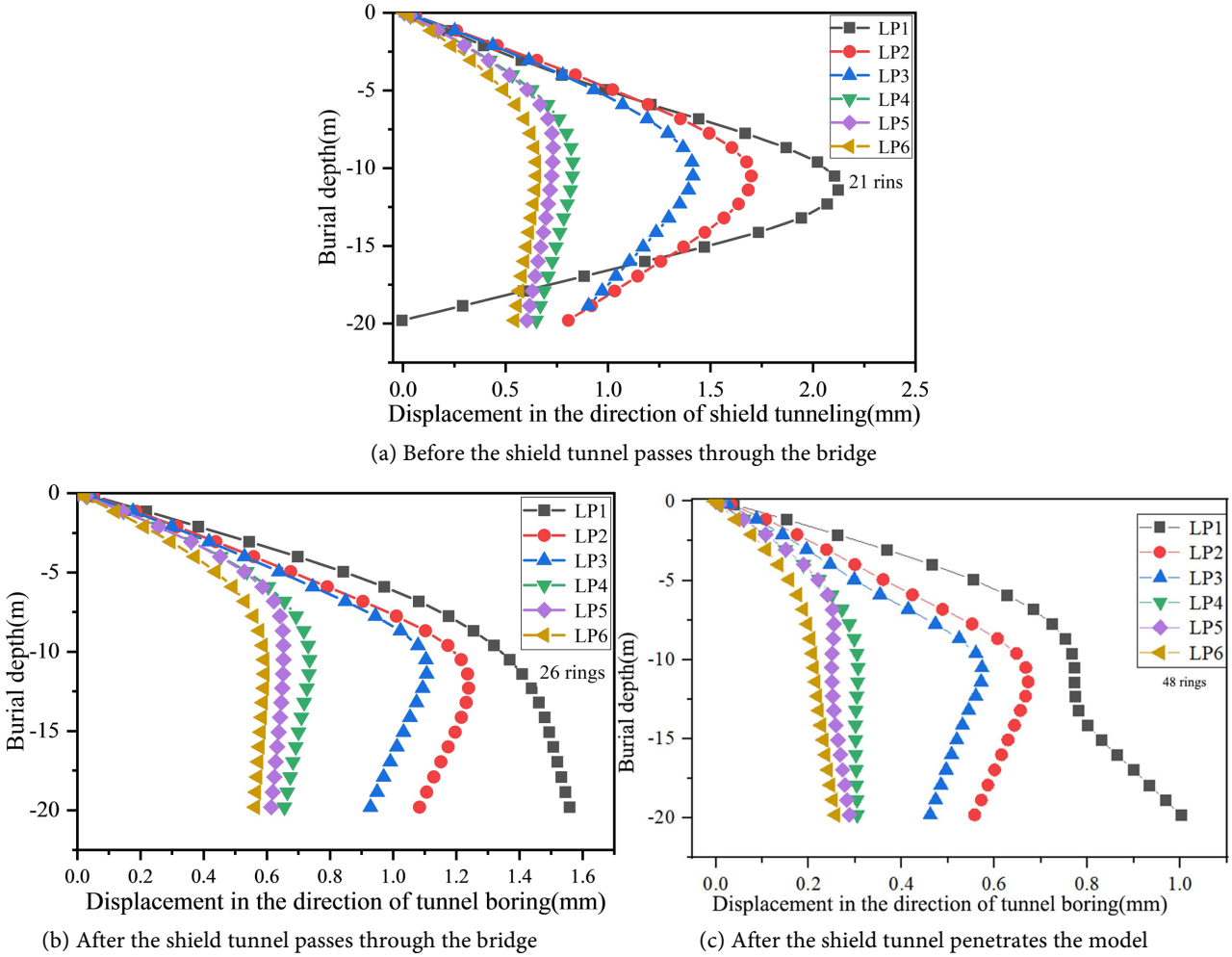

(a) Before the shield tunnel passes through the bridge

(b) After the shield tunnel passes through the bridge

(c) After the shield tunnel penetrates the model

Figure 11. Displacement diagram of a long static pile in different stages of the shield along the heading direction.

Figure 12 shows the vertical displacement cloud map of the static pressure piles, and its displacement trend is similar to that of the original piles. Due to the excavation, the initial stress field of the soil above the shield is destroyed, and the steel pipe piles near the top of the tunnel displace downwards; the piles away from the shield displace upwards under the deformation coordination of the newly built foundation, and the bottom piles also displace upwards due to the deformation coordination of the newly built foundation and their own deflection.

3.2.5. Changes in Pile Axial Force

Table 3 shows the maximum axial force of each pile before and after the shield tunneling pile grinding.

As shown in Table 3, the axial force of pile P1 decreased significantly after it was ground apart. The main load-bearing components remained the original piles, with static pressure piles LP1, LP2, and LP3, and SP1-SP4 above the shield

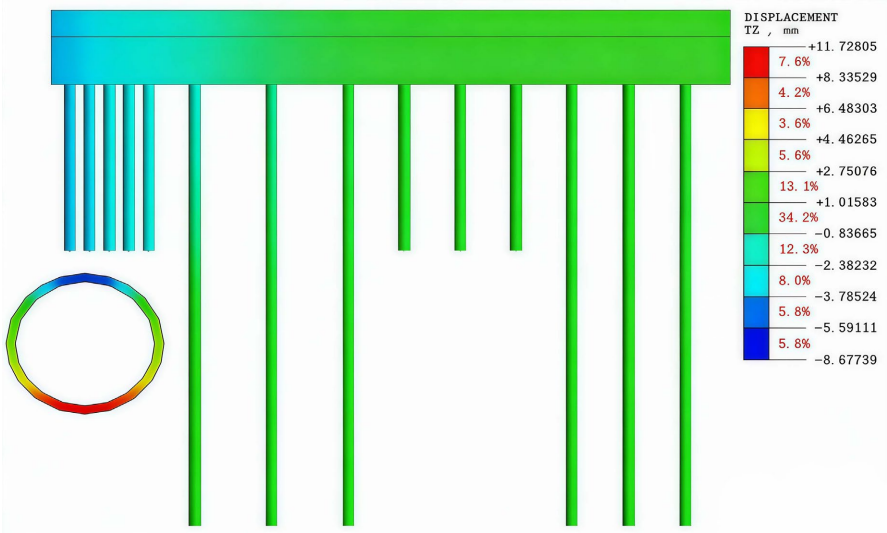

Figure 12. Cloud diagram of vertical displacement of a static pile.

Table 3. Axial force variation of each pile before and after shield construction.

Pile number	Axial force/kN		Pile number	Axial force/kN	
	Before grinding the pile	After grinding the pile		Before grinding the pile	After grinding the pile
P1	520.2	366.8	LP5	16.5	10.2
P2	1535.5	1573.6	LP6	8.4	4.3
P3	1473.7	1495.7	SP1	67.3	51.4
P4	723.3	725.5	SP2	124.7	94.9
P5	1301.1	1297.8	SP3	79.4	60.2
P6	1400.5	1391.9	SP4	58.8	42.3
LP1	257.7	405.4	SP5	50.5	36.0
LP2	98.2	138.4	SP6	102.7	104.5
LP3	80.4	94.2	SP7	93.4	93.2
LP4	12.1	6.3	SP8	50.5	50.3

tunnel bearing part of the axial force. After the shield tunneling pile grinding, the axial force of P1 decreased due to the release of soil stress, while the axial forces of P2 and P3 increased by 38 kN and 22 kN, respectively. The axial forces of static pressure piles LP1 and LP2 near the tunnel increased significantly, by 148 kN and 40 kN, respectively. The axial forces of the short static pressure piles above the tunnel decreased slightly, similar to P1, while the axial forces of piles farther from the tunnel fluctuated only slightly. It is evident that after the shield tunneling pile grinding, the bearing capacity of the ground-apart piles was impaired. The original bridge cap beams and supporting beams could adjust the axial load distribution, and the static pressure piles acted as compensating components to compensate for the bearing capacity of the damaged piles. Furthermore, the compensation

value was related to the distance from the shield tunnel; the closer the piles were to the tunnel, the stronger the compensation function.

3.2.6. Stress Response of Underpinning Beams and Cap Beams

The newly constructed pier cap is in contact with the original bridge cap beam. The shield tunneling process first affects the new pier cap; therefore, the stress of the new supporting beam is analyzed first. Before pile grinding, the new bridge-pile structure system was in equilibrium. After pile grinding, the internal forces of the pier cap changed. Figure 13 shows the stress variation of the new pier cap in the S-xx direction. When the shield tunneling removed the original pile P1, the release of soil stress caused soil settlement above the tunnel, resulting in bending deformation of the new pier cap. The upper surface near the original piles P1 and P2 changed from compression to tension, while the lower surface changed from tension to compression. This indicates that the left side of the new pier cap bent downwards. The maximum tensile stress of 0.71 MPa did not exceed the design value of the tensile strength of C40 concrete, indicating structural safety.

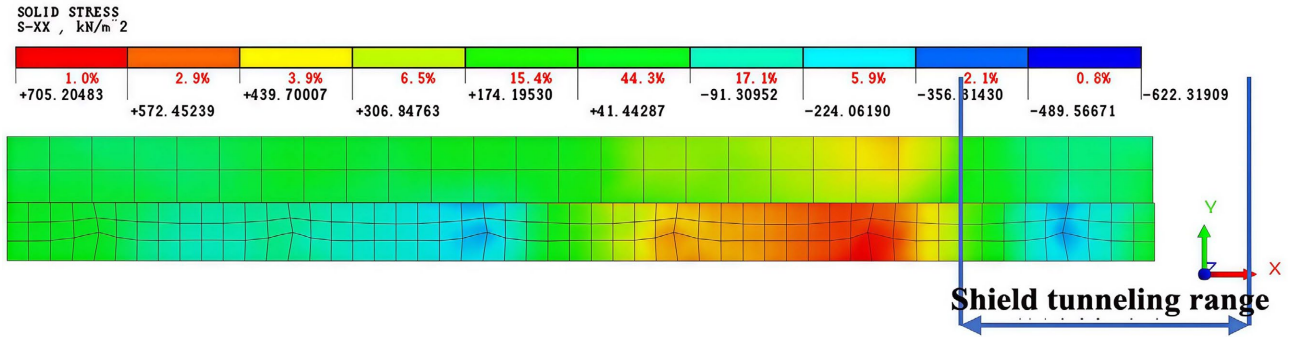

(a) upper surface of the replacement beam

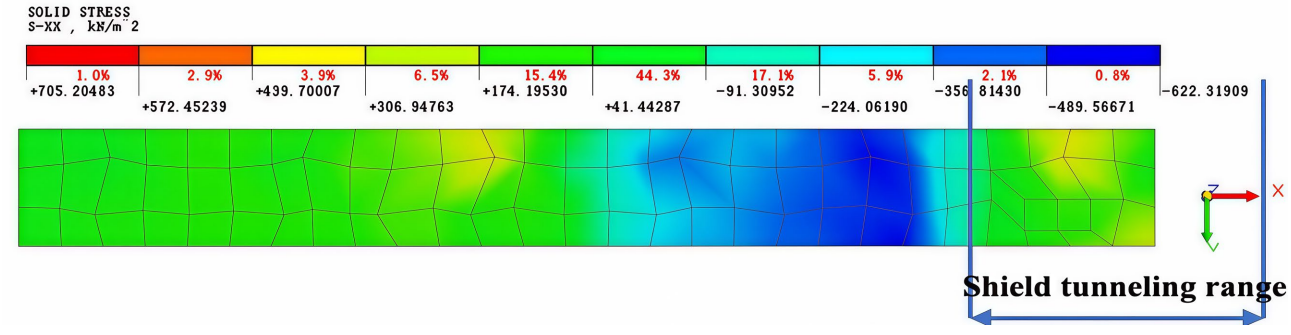

(b) underside of the support beam

Figure 13. Stress diagram in the X direction of the new cap before shield crossing.

Figure 14 shows the stress distribution of the supporting beam during the two stages of shield tunneling through the bridge and complete tunneling. As the shield tunnel advances, the stress in the newly built pier cap after the second pile cutting reaches 1.28 MPa, meeting the design requirements. When the shield moves away from the bridge, the soil stress balance is disrupted and then re-

balanced, with the stress accumulation in the newly built pier cap reaching a maximum of 1.30 MPa, also meeting the design requirements. This demonstrates that the pier cap design is safe and reliable.

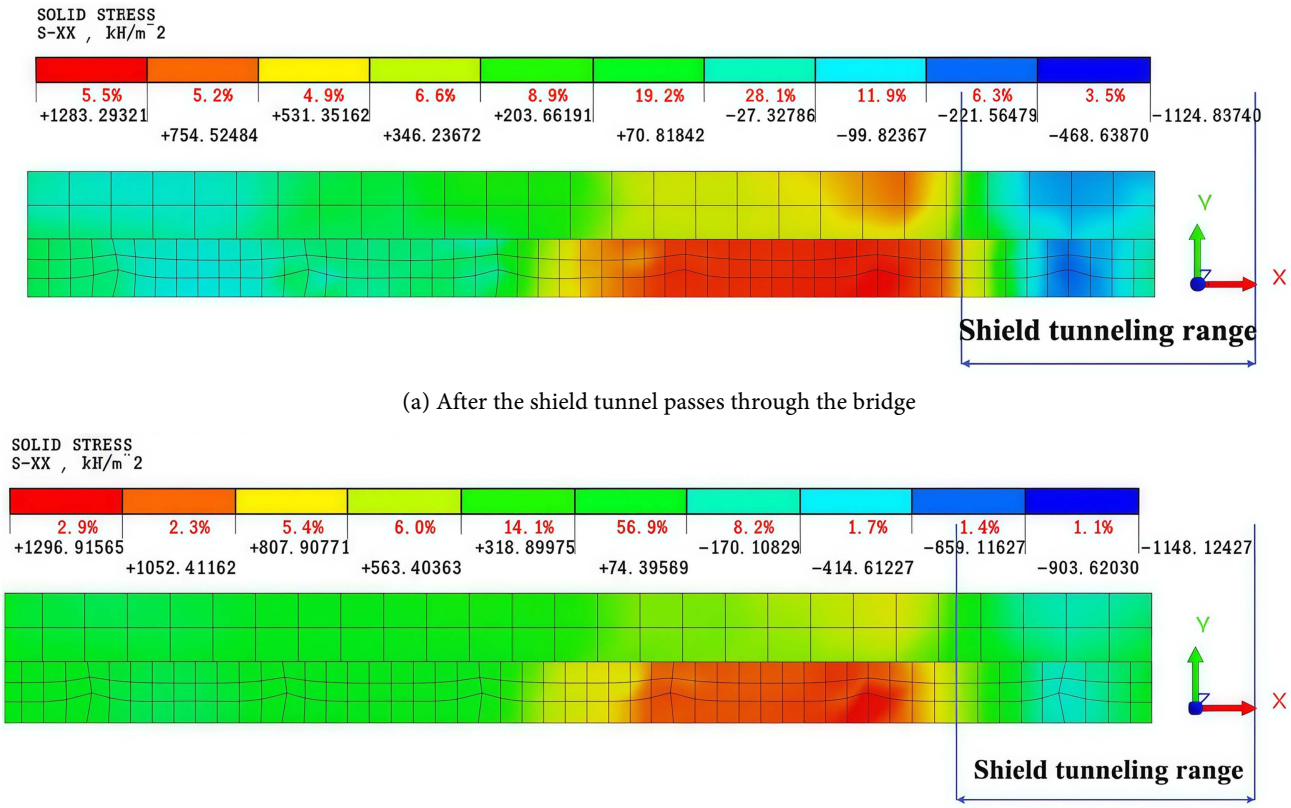

(a) After the shield tunnel passes through the bridge

(b) After the shield tunnel penetrates the model

Figure 14. Stress diagram in the X direction of the new cap at different stages of the shield.

The cap beam and the newly built support beam are in contact, and although their trends are similar, they are actually two separate components with different stresses. Figure 15 shows the stress distribution of the cap beam before and after the shield tunneling. During the shield tunneling, the absence of soil layers caused the cap beam to flex and deform. Because the newly built support beam and pile foundation system bear most of the impact of the shield tunneling, the deformation and stress of the cap beam are less than those of the support beam system. The connection between the original pile foundation and the cap beam results in significant tensile and compressive stresses inside the cap beam, with a maximum tensile stress of 234.08 kPa and a maximum compressive stress of 1284.63 kPa. At the connection between the original pile and the cap beam, these stresses are all much lower than the tensile and compressive strengths of the material, and the cap beam is stable under stress. As the shield tunneling continues, the maximum tensile stress value of the support beam increases, while the maximum tensile stress value of the cap beam does not change much, with a maximum value of 234.73 kPa near the original pile P4 position.

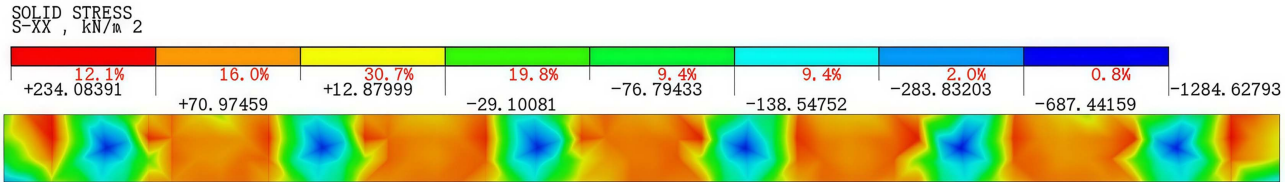

(a) Before the shield tunnel passes through the bridge

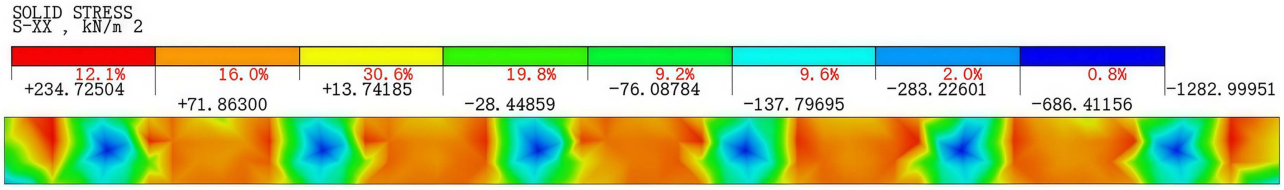

(b) After the shield tunnel passes through the bridge

Figure 15. Cloud diagram of stress variation in the X direction of the cover beam at different stages of the shield 4 Conclusions.

This paper establishes a three-dimensional finite element model based on actual engineering projects and conducts numerical simulation analysis on the pile foundation of an existing bridge through a shield tunnel. It explores surface settlement, vertical displacement of the bridge deck, displacement of the original piles and static pressure piles, changes in pile axial force, and stress response of the replacement beam, drawing the following conclusions:

1) The shield tunneling disrupts the original stress field of the soil, resulting in settlement at the top and rebound at the bottom of the tunnel. The surface settlement exhibits a "V" shape, and the minimum value of the "V"-shaped settlement trough decreases the closer it is to the bridge deck, indicating that the skin friction around the pile foundation has an inhibitory effect on reducing soil settlement. After the shield tunnel passes through, the soil reaches a new equilibrium, and simulations show that a new equilibrium state is reached 25 m after crossing the bridge.

2) The underpinning beam and cap beam play a role in deformation coordination during construction. The tunnel boring machine's passage through the bridge is a dynamic process, and its impact on the bridge-pile structure is also a dynamic equilibrium process. Calculations show that, with the coordination of the cap beam and abutment, bridge deck settlement and structural stress are small, the underpinning system is safe, and the underpinning scheme is reasonable and reliable.

3) During shield tunneling, the original piles and static pressure piles undergo flexural deformation due to the tunneling pressure and grouting pressure. Most of the pile deformation recovers as the shield moves away. Under the combined action of tunneling pressure and lateral compression, the piles displace and deform along the direction of the resultant force. Since the resultant force is influenced by multiple factors, horizontal load analysis of the pile foundation is necessary during the shield tunneling phase, and the underpinning process must ensure the piles' stiffness against lateral deformation.

4) During the tunnel boring machine pile driving process, the soil above the tunnel settles, generating negative skin friction due to the coordinated deformation of the pier cap and the influence of residual piles. This ground loss causes a reversal of the stress on the cap beam and supporting beam structural system. Conventional bridge structural designs do not consider this situation, necessitating a re-examination of the stress on the newly constructed pier cap and cap beam, and an assessment of whether structural reinforcement or strengthening is required.

Conflicts of Interest

The authors declare no conflicts of interest regarding the publication of this paper.

References

[1] Lv, J., Lin, D., Wu, W., Huang, J., Li, Z., Fu, H., *et al*. (2022) Mechanical Responses of Slurry Shield Underpassing Existing Bridge Piles in Upper-Soft and Lower-Hard Composite Strata. *Buildings*, **12**, Article 1000. https://doi.org/10.3390/buildings12071000

[2] Zhang, J., Zhao, M., Liu, H. and Xu, X. (2013) Networked Characteristics of the Urban Rail Transit Networks. *Physica A*: *Statistical Mechanics and its Applications*, **392**, 1538-1546. https://doi.org/10.1016/j.physa.2012.11.036

[3] Tang, R., Lin, B. and Liang, P. (2019) Safety Study on Direct Pile Cutting of Shield Underneath a Residential Building. *Journal of Underground Space and Engineering*, **15**, 878-883.

[4] Wei, G., Yang, B., Wu, H., *et al*. (2020) Research on Longitudinal Deformation of Existing Shield Tunnel Caused by Shield Tunneling. *Chinese Journal of Underground Space and Engineering*, **16**, 1754-1762+1808.

[5] Makarchian, M. and Poulos, H.G. (1996) Simplified Method for Design of Underpinning Piles. *Journal of Geotechnical Engineering*, **122**, 745-751. https://doi.org/10.1061/(asce)0733-9410(1996)122:9(745)

[6] Jin, F., Xu, Q., Ma, Z., Ma, J. and Ming, J. (2012) Study on the Length of Excavation Exposure during Pile Replacement under Bridges. *Journal of Underground Space Engineering*, **8**, 396-403.

[7] Vynnykov, Y.L., Kharchenko, M.O. and Manzhalii, S.M. (2021) Reinforcement of a Deformed Structure on the Pile Foundation. *IOP Conference Series*: *Materials Science and Engineering*, **1021**, Article 012030. https://doi.org/10.1088/1757-899x/1021/1/012030

[8] Zhao, X., Zhang, T., Liu, S., *et al*. (2022) Analysis of Shaped Bearing Pile Foundation Buttress Construction and Its Safety. *Construction Technology* (*in Chinese and English*) *Magazine*, 334-337.

[9] Ma, L. and Wang, J. (2012) Technology of Pile Foundation Underpinning in Shield Tunnel of Xi'an Subway. *Applied Mechanics and Materials*, **204**, 1445-1448. https://doi.org/10.4028/www.scientific.net/amm.204-208.1445

[10] Xu, Q., Zhu, H., Ma, X., *et al*. (2012) Study on the Replacement and Pile Removal Technology of Group Pile Foundation Underneath an Underpass Shield Tunnel Crossing a Bridge. *Journal of Geotechnical Engineering*, **34**, 1217-1226.

[11] Li, D., Qian, J., Wu, S., *et al*. (2012) Finite Element Analysis of Deformation of Exist-

ing Buttress Piles under Excavation. *Journal of Geotechnical Engineering*, **34**, 238-242.

[12] Deng, T., Guan, Z., Chen, K., *et al*. (2015) Simplified Calculation of Jacking Load in Active Buttressing of Bridge Pile Foundation. *Geotechnics*, **36**, 3259-3267.

[13] Zhang, C., Zhao, Y., Zhang, Z. and Zhu, B. (2021) Case Study of Underground Shield Tunnels in Interchange Piles Foundation Underpinning Construction. *Applied Sciences*, **11**, 1611-1612. https://doi.org/10.3390/app11041611

[14] Cheng, P., Xu, Q., Li, G. and Li, X. (2018) Influence on High-Speed Railway Bridge Caused by Shield Tunneling in Sandy Pebble Stratum and Its Controlling Technologies. *Transportation Research Congress* 2016: *Innovations in Transportation Research Infrastructure*, Reston, 6-8 June 2016, 507-520. https://doi.org/10.1061/9780784481240.052

[15] Stulgis, R.P., Barry, B.E. and Harvey, Jr., F.S. (2004) Foundation Underpinning with Mini-Piles: "A First" in Guyana, South America. *GeoSupport* 2004, Orlando, 29 December 2004, 700-711. https://doi.org/10.1061/40713(2004)15

[16] Horpibulsuk, S., Kumpala, A. and Katkan, W. (2008) A Case History on Underpinning for a Distressed Building on Hard Residual Soil Underneath Non-Uniform Loose Sand. *Soils and Foundations*, **48**, 267-285. https://doi.org/10.3208/sandf.48.267

[17] Ishimura, T., Metoki, M. and Shimizu, M. (2006) Development of Removed Pile Method with Cutting. *Tunnelling and Underground Space Technology*, **21**, 411-412. https://doi.org/10.1016/j.tust.2005.12.058

[18] van Hasselt, D.R.S., Hentschel, V., Hutteman, M., Kaalberg, F.J., van Liebergen, J.C.G., Netzel, H., *et al*. (1999) Amsterdam's North/South Metroline. *Tunnelling and Underground Space Technology*, **14**, 191-210. https://doi.org/10.1016/s0886-7798(99)00033-4

[19] Iwasaki, Y., Watanabe, H., Fukuda, M., Hirata, A. and Hori, Y. (1994) Construction Control for Underpinning Piles and Their Behaviour. *Géotechnique*, **44**, 681-689. https://doi.org/10.1680/geot.1994.44.4.681

[20] Yamaguchi, I., Yamazaki, I. and Kiritani, Y. (1998) Study of Ground-Tunnel Interactions of Four Shield Tunnels Driven in Close Proximity, in Relation to Design and Construction of Parallel Shield Tunnels. *Tunnelling and Underground Space Technology*, **13**, 289-304. https://doi.org/10.1016/s0886-7798(98)00063-7